Chemical Physics Letters 462 (2008) 31–34

Contents lists available at ScienceDirect

Chemical Physics Letters

journal homepage: www.elsevier.com/locate/cplett

Deep-UV absorption and Rayleigh scattering of carbon dioxide

D. Ityaksov [a,*], H. Linnartz [a,b], W. Ubachs [a]

[a] Laser Centre Vrije Universiteit Amsterdam, Depatment of Atomic, Molecular and Laser Physics, De Boelelaan 1081, NL 1081 HV, Amsterdam, Netherlands
[b] Raymond and Beverly Sackler Laboratory for Astrophysics, Leiden Observatory, PO. Box 9513, NL 2300 RA, Leiden, Netherlands

ARTICLE INFO

Article history:
Received 24 April 2008
In final form 11 July 2008
Available online 22 July 2008

ABSTRACT

Cavity ring-down spectroscopy and pressure ramp measurements have been used to determine the extinction coefficients of CO_2 in the deep-ultraviolet wavelength region, between 198 and 270 nm. The observed optical extinction confirms that there is a clear absorption onset of CO_2 in the deep-UV wavelength region. This onset has been reported previously around 205 nm. The new set of measurements presented here shows that the onset actually starts at higher energy, around 202 nm. For longer wavelengths it is found that the optical extinction demonstrates a $1/\lambda^4$ like behavior, as typical for Rayleigh scattering.

1. Introduction

At deep-UV wavelengths light scattering becomes much stronger due to a $1/\lambda^4$ scaling of the Rayleigh scattering. The case of CO_2 is special as a number of studies also report an absorption onset between 200 and 205 nm [1,2]. The exact onset of this absorption is important to model the photochemistry of planetary atmospheres that are rich of carbon dioxide, including that of the Earth and Mars. However, the exact wavelength where the CO_2 absorption onset steeply starts has been a topic of dispute, in particular due to a data set by Ogawa [3], which was suggestive of an absorption onset near 220 nm, just above the dissociation limit of CO_2. The most recent measurements by Karaiskou et al. [4] providing accurate cross-sections in the wavelength range 200–206 nm at room temperature as well as at 373 K may have settled this issue, showing that the findings of Ref. [4] must be in error. They find an onset for absorption around 205 nm for carbon dioxide. Proceeding to shorter wavelengths the extinction cross-section of CO_2 increases by several orders of magnitude in the range 200–120 nm [2,5].

In this study we present an extensive series of new data points in the 198–205 nm region where the onset is expected, combining pressure ramp measurements and cavity ring-down spectroscopy at deep-UV wavelengths [6]. Our results confirm the Karaiskou et al. conclusion that the Ogawa data must be in error. At longer wavelengths in the range 215–270 nm extinction is measured and compared to Rayleigh scattering cross-sections previously obtained, either through direct cross-section measurements [7,8] or through derivation from the index of refraction [9], where also the effect of depolarization is included [10]. Based on the combined data sets an updated functional representation of the wavelength dependent Rayleigh scattering cross-section $\sigma_R(\lambda)$ is derived.

The present quantitative study of the CO_2 extinction in a wide wavelength region yields further insight in the absorption onset. This is important in an atmospheric context, since it is the combined effect of light scattering, photo-absorption and photo-processing that determines the impact of deep-UV light on atmospheric CO_2. In addition the atmospheric extinction determines the penetration of deep-UV light to the lower layers in the atmosphere, where it may cause photo-decomposition of other relevant species.

2. Analytical approach

Rayleigh scattering can be measured by detecting the *extinction* from a light beam (along a length z or during a time t) as given by Beer's law,

$$I = I_0 \exp(-N\sigma z) = I_0 \exp(-N\sigma c t) \quad (1)$$

where I_0 is the intensity at $z = 0$ and $t = 0$, N is the density of the molecules and σ is the value of the extinction cross-section that accounts for *both* scattering σ_R and absorption σ_A contributions and c is the speed of light. More specifically, the Rayleigh scattering cross-section is given (in units of cm^2 per molecule) by

$$\sigma_R = \frac{24\pi^3}{\lambda^4 N^2}\left(\frac{n(\lambda)^2 - 1}{n(\lambda)^2 + 2}\right)^2 F_k(\lambda) \quad (2)$$

where λ is the wavelength in cm, N is the density of the molecules in cm^3 and $n(\lambda)$ is the wavelength dependent refractive index. The dimensionless King correction factor $F_k(\lambda)$ accounts for the anisotropy in the scattering by non-spherical molecules. Eq. (2) relates the Rayleigh scattering cross-section to two directly measurable quantities, the refractive index and the gas density. Hence, a comparison between direct measurements of the Rayleigh scattering

* Corresponding author. Fax: +31 20 59 87 992.
E-mail address: ityaksov@few.vu.nl (D. Ityaksov).

0009-2614/$ - see front matter © 2008 Elsevier B.V. All rights reserved.
doi:10.1016/j.cplett.2008.07.049

cross-section with measurements of the refractive index yields information on $F_k(\lambda)$. In addition, this factor is obtained via depolarization measurements in Raman scattering or via *ab initio* calculations of molecular properties. For CO_2 this wavelength dependent parameter is available from literature [10] and given by

$$F_k(\lambda) = 1.14 + \frac{25.3 \times 10^{-12}}{\lambda^2} \tag{3}$$

Dispersion formulas for the refractive index and the depolarization of atmospheric gases are generally available from literature and for CO_2 specifically given by [9]

$$n(\lambda) - 1 = 1.1427 \times 10^6 \left(\frac{5799.3 \cdot \lambda^2}{16.6 \cdot 10^9 \cdot \lambda^2 - 1} + \frac{120 \cdot \lambda^2}{7.96 \times 10^9 \cdot \lambda^2 - 1} + \frac{5.33 \cdot \lambda^2}{5.63 \times 10^9 \cdot \lambda^2 - 1} + \frac{4.32 \cdot \lambda^2}{4.6 \times 10^9 \cdot \lambda^2 - 1} + \frac{1.22 \times 10^{-5} \cdot \lambda^2}{5.85 \times 10^6 \cdot \lambda^2 - 1} \right) \tag{4}$$

In Eqs. (3) and (4) the wavelength λ (in vacuum) is given in cm. Alternatively, a direct determination of σ_R via extinction measurements provides a test of the calculated Rayleigh scattering cross-section. Sneep and Ubachs verified in a range of visible wavelengths (near 475 nm, at 532 nm and near 560 nm) that the Rayleigh cross-section as obtained from extinction measurements is in agreement with results from dispersion and depolarization data [8].

3. Experimental approach

The experimental approach is based upon cavity ring-down (CRD) detection of a series of pressure ramp measurements, a method developed by Naus and Ubachs [11]. The pressure ramp procedure allows distinguishing the linear extinction signal, associated with molecular scattering and absorption, from a wavelength-dependent background due to variations in mirror reflectivity or due to a quadratic dependence resulting from collisionally induced phenomena [12]. For this it is necessary that the laser frequency is kept constant. Details on the experimental setup, the pressure ramp method and the extension of CRDS-techniques to deep-UV wavelengths are available from [6,7,11,12].

The present measurements are performed in two distinct wavelength regions (the 215–270 nm interval and the 198–204 nm interval). The laser bandwidth in this regime is better than 0.2 cm^{-1}. Wavelengths are chosen according to the availability of high-reflectivity mirrors and listed in Table 1. The reflectivity of the cavity ring-down mirrors is better than 99.4% in the 215.38–270.15 nm region and ~98% at 210.12 nm. An effective reflectivity of 99.2% is achieved in the deep-UV region of 198–201 nm. For the 215–270 nm interval the radii of curvature of available mirrors prompted the use of a relatively short cell, at an optimal cavity length of 40 cm. In these experiments the resulting decay times amount to about 250 ns and are determined by a non-linear least-squares fitting with about 5% uncertainty. The 1 m focal distance of the mirrors for 200 nm makes it possible to use a special 82 cm long CRD cell, previously designed for pressure ramp studies [11,12]. It contains a large number of inlet holes for the gas to enter the scattering region, while avoiding turbulence effects.

In cases, where the laser line-width applied in the CRD scheme is negligible with respect to the molecular extinction feature, experimental decay times can be directly converted into absolute cross-sections [13]. The decay rate β obtained in a CRDS measurement, equaling the inverse of the ring-down decay time τ, scales with the gas density

Table 1
Extinction cross-section values in the 197.7–270.15 nm region, obtained from CRD pressure-ramp measurements and calculated Rayleigh scattering cross-sections values σ_R^{calc} in CO_2

λ (nm)	$\sigma_R^{calc}/10^{-25}$ (cm^2)	$\sigma^{measured}/10^{-25}$ (cm^2)
197.70	10.1	52.7 ± 2.2
197.84	10.0	51.4 ± 1.5
198.28	9.9	54.9 ± 1.9
198.38	9.9	43.2 ± 1.7
198.48	9.9	49.2 ± 2.4
198.75	9.8	32.1 ± 3.4
199.10	9.7	33.5 ± 3.5
199.55	9.6	24.0 ± 2.6
199.90	9.5	23.9 ± 0.7
200.08	9.5	30.0 ± 0.9
200.42	9.4	23.0 ± 3.0
200.76	9.3	16.9 ± 1.0
201.00	9.3	15.5 ± 1.6
201.33	9.2	12.6 ± 1.1
201.58	9.2	10.1 ± 1.3
201.78	9.1	8.0 ± 1.2
202.43	9.0	7.9 ± 0.8
203.11	8.8	7.8 ± 1.6
203.76	8.7	7.5 ± 1.5
215.38	6.7	6.6 ± 1.0
251.72	3.2	3.3 ± 0.5
270.15	2.4	2.3 ± 0.4

$$\beta = \frac{c|\ln R(\lambda)|}{d} + c\sigma N \tag{5}$$

Hence, from a series of measurements at fixed wavelength and at increasing gas density N, both the averaged reflectivity $R(\lambda)$ of the mirror set and the absolute extinction cross-section σ can be obtained. Note that the latter follows from the slope of each β vs. N measurement and that the resulting value is independent of the cell length d. In the present study CRD pressure-ramp scans are recorded in pressure ranges between 0 and 10^5 Pa, i.e. up to atmospheric pressure. All measurements have been taken at room temperature. The empirical relations given here are for 288.15 K and 101 325 Pa.

The wavelength of the laser is kept fixed during a pressure ramp measurement. Both the pressure and the decay time of the cavity are continuously monitored, while gradually increasing the gas density in the scattering region. At every momentary pressure value, five decay transients are digitized and fitted. The precise value of the pressure inside the ring-down cell is measured simultaneously with 0.15% accuracy by a pressure sensor. High purity gases are used (99.7% for CO_2) and a 0.5 μ filter cleans the injected gas from dust and aerosol particles, which may affect the scattering properties of the gas.

4. Results and discussion

The results of the measurements performed at 22 distinct wavelengths between 197.7 and 270.15 nm are listed in Table 1. The behavior of the experimentally obtained extinction cross-sections as well as a comparison with existing data is given in Fig. 1. The slope coefficient of each individual measurement is determined with an accuracy of a few percent. The experimental error (1σ uncertainty) is ~15% for the measurements in the 215.38–270.15 nm interval and about 10% for observations in the wavelength region where the turbulence free CRD cell has been used. A significant number of pressure-ramp scans had to be taken to decrease the experimental error. In none of the experiments performed signatures of quadratic density dependence were found. From this result we conclude that CO_2–CO_2 collision-induced phenomena do not play a role, for the wavelength region covered and for pressures below 1 atmosphere.

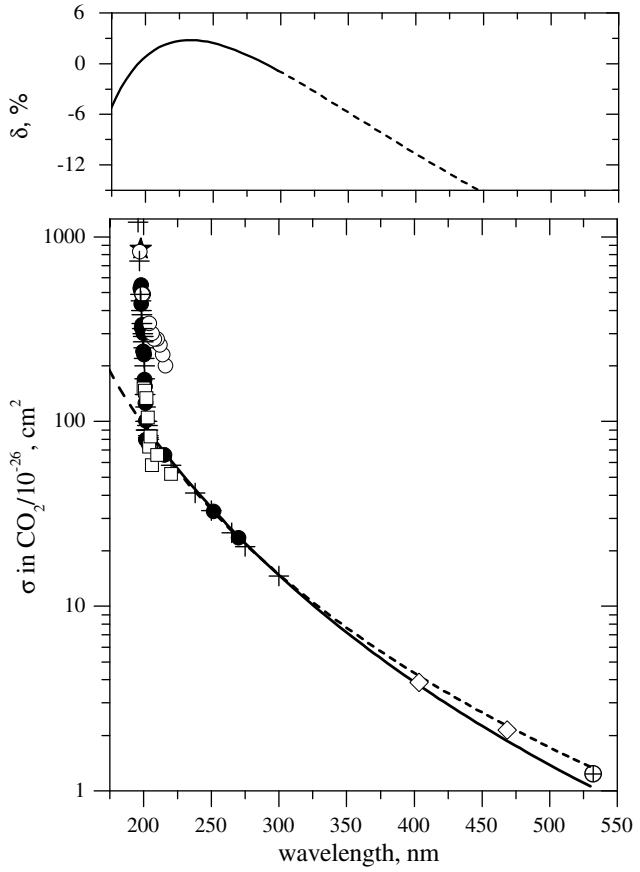

Fig. 1. Results from extinction measurements in CO_2. The lower trace shows the experimental data points as presently measured in this work (black circles) and those available from literature. Crossed open circles corresponds to Sneep and Ubachs [7], black stars to Sneep et al. [6], open circles to Ogawa [3], vertical crosses to Shemansky [1], open squares to Karaiskou et al. [4] and diamonds to Dong and Gupta [8]. The solid black line corresponds to a fit with $\bar{\sigma} = 1.78(7) \times 10^{-46}$ and $\varepsilon = 0.625(3)$ and the dashed line corresponds to a Rayleigh scattering cross-section simulation extrapolated to the visible domain, using the dispersion formula available from [9] and depolarization from [10]. The difference between these two graphs is shown in the upper panel.

The predicted values of the Rayleigh scattering cross-sections in CO_2 are obtained from the dispersion formulas for the refractive indices [9] and depolarization ratios [10]. The calculated Rayleigh scattering cross-sections and measured extinctions, as well as their errors (1σ uncertainties) are listed in Table 1.

Due to the wavelength dependence of the refractive index and the King correction factor, the Rayleigh scattering cross-section is not exactly proportional to $1/\lambda^4$ and a proper mathematical function accounting for this difference (see Refs. [7,11]) has to be used

$$\sigma_R = \bar{\sigma} \nu^{(4+\varepsilon)} \tag{6}$$

where ν is the light frequency in cm^{-1}. Hence the wavelength-dependent Rayleigh scattering σ_R is expressed in terms of two variables $\bar{\sigma}$ and ε. A two step fitting procedure has been applied in which the $\bar{\sigma}$ parameter is kept fixed to the predicted and uncorrected theoretical value (calculated from the refractive index and the King correction factor), while the value for ε is repeatedly optimized. During the second step, free and fixed parameters are interchanged and statistically reliable values are found after a few iterations. A non-linear least-squares fit to Eq. (6) has been performed for all data points, as available from this work and from literature – apart from the older data by Ogawa [3] covering the range 202–300 nm. In the wavelength domain from 202 to 300 nm this yields values $\bar{\sigma} = 1.78(7) \times 10^{-46}$ and $\varepsilon = 0.625(3)$. Note that in this representation ε is dimensionless and the dimension of $\bar{\sigma}$ depends on the value of ε and therefore is not specified.

In Fig. 1 the data pertaining to this fit to the Rayleigh scattering data (fit performed in the interval 202–300 nm) is shown (full line), as well a calculation based on dispersion and depolarization ratios (dashed line). In the upper part of the figure a deviation between both representations is given, showing that in the range 202–300 nm the agreement is within a few %, while for $\lambda > 300$ nm there is a gradually increasing discrepancy up to 20% at the longest included wavelength (532 nm). This discrepancy can be ascribed to the fact that the fit determining $\bar{\sigma}$ and ε is restricted to UV wavelengths, i.e. it is not meant to be extrapolated beyond 300 nm. Note that the Rayleigh scattering in CO_2 for the range of visible wavelengths is represented by largely differing parameters [7]. The measurements on the index of refraction in Ref. [9] represent data in the deep-UV range, covering the interval 180–254 nm (distinct atomic line emissions are used in their experiment), hence the dashed line in Fig. 1 is an extrapolation. Considering this, the agreement between directly measured and calculated Rayleigh cross-sections is rather good; within a few % in the relevant range.

The data of Bideau-Mehu et al. on the index of refraction [9] imply that the Rayleigh scattering cross-section is represented down to 180 nm by Eqs. (2)–(4). Hence the sudden increase in Fig. 1 clearly is representative for the absorption onset in CO_2. This onset is shown in more detail, and on a linear scale for the extinction in Fig. 2, where data by Shemansky [1], Ogawa [3], Sneep et al. [6], Karaiskou et al. [4] and Lewis and Carver [5] are plotted together with the present data. Overall agreement between the data sets

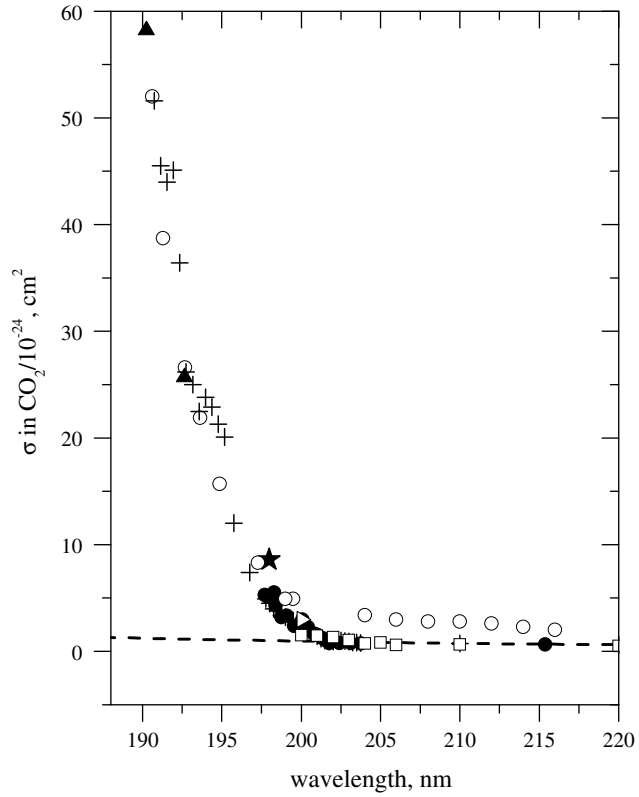

Fig. 2. Illustration of the absorption onset in CO_2, as derived in this study (black circles) and observed in other work. Vertical crosses are from Shemansky [1], the open triangle is from Parkinson et al. [2], the open circles are from Ogawa [3], the open squares are from Karaiskou et al. [4], solid triangles from Lewis and Carver [5] and the black star is from Sneep et al. [6]. The dashed line represents the Rayleigh scattering cross-section simulation extrapolated to the visible domain, using the dispersion and depolarization formulas available from [9,10].

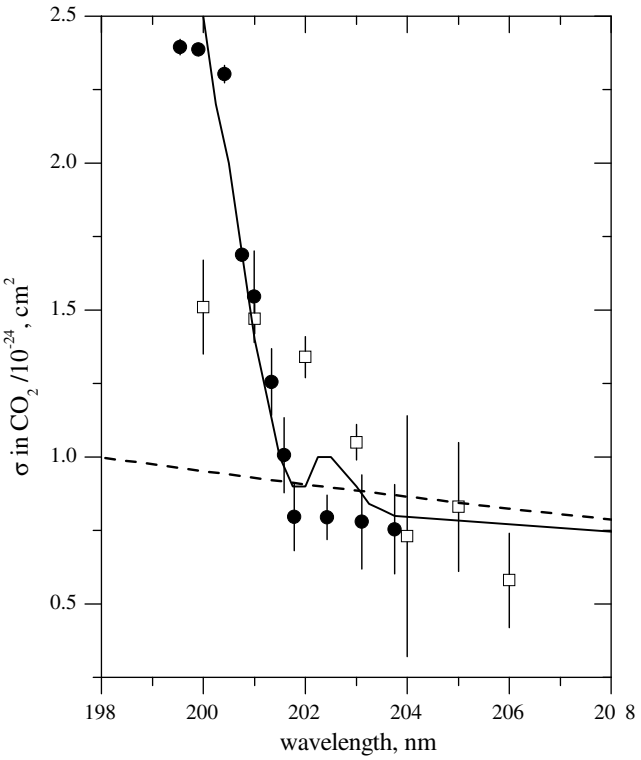

Fig. 3. Illustration of the absorption onset in CO_2, as derived in this study (black circles) and observed in other work. Solid line represents the data by Shemansky [1], the open squares are from Karaiskou et al. [4].

is found, except for the data by Ogawa [3]. At the short wavelength side the data by Shemansky [1] can be matched to those of Lewis and Carver [5] and of Parkinson et al. [2], showing a strong increase of the absorption from the Rayleigh scattering level below 10^{-24} cm^{-2} to a plateau in the broad absorption resonance near 130–150 nm at a cross section level of 10^{-18} cm^2.

To further clarify details of the absorption onset, we have magnified the scales of Fig. 2 around the onset point as shown in Fig. 3. In previous reports the absorption onset in carbon dioxide has been put around 205 nm [4]. The large number of measurements in this region indicates that the actual onset starts at a value of about 202 nm. A comparison of the existing data sets in the 200–205 nm region shows that our data are very complementary with the Shemansky results [1], whereas the Karaiskou data yield only slightly higher values. The spread in the three data sets that now reaches agreement in the range 200–205 nm (present data, Karaiskou et al. [4] and Shemansky [1]) is rather large, being up to 20%. We note that this is the range where absorption is governed by vibrationally excited CO_2, making the extinction cross-section strongly dependent on temperature, as was verified in the experiments by Karaiskou et al. Moreover the spread demonstrates that this part of the deep-UV spectrum is a difficult region to perform experiments at high accuracy.

At wavelengths in the range 197.7–200 nm the data show signature of an oscillatory behavior, reminiscent of a vibrational structure. This structure was more clearly observed in the 180–190 nm interval by Parkinson et al. [2]. In principle, the high resolution of the present setup would allow for unraveling these oscillations if data were collected at much smaller wavelength steps. Although this is very time consuming when applying the pressure-ramp method, it may be a topic for further study.

Near 200 nm, there is a slightly increased penetration of deep-UV to lower layers in the Earth's atmosphere [14], due to a gap between the strong extinctions produced by the O_2 molecule (shortward of 200 nm) and the O_3 molecule (longward of 210 nm). The onset of absorption by carbon dioxide in this wavelength interval may be of importance for a detailed modeling of the photo-physics and chemistry in the stratospheric layer of the Earth's atmosphere.

5. Conclusion

Through deep-UV extinction measurements and the technique of cavity ring-down spectroscopy in a wide wavelength range further clarity has been obtained on the deep-UV onset of absorption in the CO_2 molecule. The onset is found close to 202 nm, while also a model description for the Rayleigh scattering cross-section for the entire UV range is presented.

Acknowledgments

The authors thank Gijs Vollenbroek for assisting in setting up the deep-UV laser system, Jacques Bouma for technical support and The Netherlands Foundation for Fundamental Research (FOM) for financial support via their Molecular Atmospheric Physics (MAP) program.

References

[1] D.E. Shemansky, J. Chem. Phys. 56 (1972) 1582.
[2] W.H. Parkinson, J. Rufus, K. Yoshino, Chem. Phys. 290 (1990) 251.
[3] M. Ogawa, J. Chem. Phys. 54 (1974) 2550.
[4] A. Karaiskou, C. Vallance, V. Papadakis, I.M. Vardavas, T.P. Rakitzis, Chem Phys. Lett. 400 (2004) 30.
[5] B.R. Lewis, J.H. Carver, J. Quant. Spectr. Rad. Transfer 30 (1983) 297.
[6] M. Sneep, S. Hannemann, E.-J. van Duijn, W. Ubachs, Opt. Lett. 29 (2004) 1378.
[7] M. Sneep, W. Ubachs, J. Quant. Spectr. Rad. Transfer 92 (2005) 293.
[8] F. Dong, M. Gupta, Sens. Actuators, B 129 (2008) 158.
[9] A. Bideau-Mehu, Y. Guern, R. Abjean, A. Johannin-Gilles, Opt. Commun. 9 (1973) 432.
[10] G.R. Alms, A.K. Burnham, W.H. Flygare, J. Chem. Phys. 63 (1975) 3321.
[11] H. Naus, W. Ubachs, Opt. Lett. 25 (2000) 347.
[12] M. Sneep, D. Ityaksov, I. Aben, H. Linnartz, W. Ubachs, J. Quant. Spectr. Rad. Transfer 98 (2006) 405.
[13] H. Naus, I.H.M. van Stokkum, W. Hogervorst, W. Ubachs, Appl. Opt. 40 (2001) 4416.
[14] R.R. Meier, Space Sci. Rev. 58 (1991) 1.